Ronchi test with equivalent wavelength

Anmi García-Arellano,[1,*] Fermín Granados-Agustín,[1] Manuel Campos-García,[2]
and Alejandro Cornejo-Rodríguez[1]

[1]Departamento de Óptica, Instituto Nacional de Astrofísica, Óptica y Electrónica Sta. Ma. Tonantzintla, Puebla, 72000 México

[2]Centro de Ciencias Aplicadas y Desarrollo Tecnológico, Universidad Nacional Autónoma de México. Circuito exterior S/N,
Ciudad Universitaria, A. P. 70–186, Delegación Coyoacán, C.P.04510, México D.F., México

*Corresponding author: gaanmi@inaoep.mx

In this work we present an experimental proposal to evaluate optical surfaces with high slopes or with infrared wavelengths based on the Ronchi test as well as on the concept of equivalent wavelength. A spatial modulator is used in the implementation of the Ronchi test, and a white LED with different color filters is employed in order to generate different wavelengths. Two Ronchigrams with incoherent light, each one for a different color, are registered and computationally processed, thus generating a third one with an equivalent wavelength. The results obtained show that it is possible to generate patterns with traditional rulings and substructured sequences of Katyl. Additionally, we discuss some of the limitations of employing different rulings. Finally, we found that appropriate image enhancing algorithms allow us to improve the visibility of the resulting fringes and thus obtain a better analysis.   © 2012 Optical Society of America

OCIS codes: 120.0120, 220.0220.

1. Introduction

Some of the limitations of interferometry with a single wavelength appear when measuring surfaces that vary rapidly in height or when evaluating surfaces with high slopes [1–3]. In the first case, the fringe density generated commonly exceeds the resolution of conventional CCDs, while in the second case, the determination of the fringe order becomes a difficulty. Then, the employment of a longer wavelength becomes an option in order to overcome these difficulties. Aspherical surfaces are an example of this kind of surface [4], which has always been difficult to evaluate with traditional interferometry, and evaluation with masters is expensive when there is a unique piece to analyze.

On the other hand, when we work with surfaces at infrared wavelengths, we have the requirement of wavelengths longer than usual ($\lambda = 633$ nm) as well

as the availability of all the corresponding optics for this wavelength [1].

According to the ideas presented in [5,6], some authors [1,7,8] proposed the use of a combination of two wavelengths in interferometric techniques in order to obtain results as if a unique larger wavelength were used. The proposal consists of illuminating the surface under test with two coherent beams of different wavelengths, in order to generate a pattern with a beat wavelength [7], but the illumination can be also carried out separately, and then by proper processing the pattern for the beat wavelength can be obtained [3,9,10]. This process requires a filtering procedure to select the desired frequency.

Based on the idea of equivalent wavelength, we present a new alternative to solve the problem of evaluating the type of surfaces described above. Instead of using traditional interferometry, we propose to employ the Ronchi method as the evaluation test, for which the employment of a low period Ronchi ruling is required for the generation of a pattern with equivalent wavelength. This testing method is

insensitive to local perturbations and allows the use of incoherent light. In fact, if an LCD is employed, the advantages of this system are the ability to rapidly change the characteristics of the ruling, which is useful in the fabrication processes, and its insensitivity to small perturbations that can affect the results when working in environments outside the laboratory. These advantages make this proposal attractive for testing during different fabrication stages that require a robust test in order to quickly predict the areas to be polished.

This paper is organized as follows. Section 2 presents the principal ideas of the Ronchi test and the synthetic fringe pattern formation previously described in [11]. Section 3 describes the digital image processing (DIP) techniques employed to combine two Ronchigrams in order to enhance and to filter the generated beat Ronchigram. Section 4 presents the experimental array employed and the Ronchigrams with equivalent wavelength obtained in this work. Finally, concluding remarks and some comments on the improvement of the proposal are presented.

2. Theory

A. Ronchi Test

With this technique, it is possible to obtain information of the *transverse aberration* of a surface under test [12]. A schematic of the experimental arrangement is shown Fig. 1. The implementation of this testing procedure consists of using a ruling of certain frequency, composed of parallel and equidistant dark and transparent apertures. Then, by looking through the ruling, an interference pattern can be observed, produced by shear of the wavefronts passing by the Ronchi ruling.

The mathematical treatment to understand the test as a lateral sheared interferometer is based on Fourier theory. According to Fig. 2, the description of the Ronchi test is as follows. $F_0(x_0, y_0)$ represents the wavefront at the exit pupil and is defined as [12]
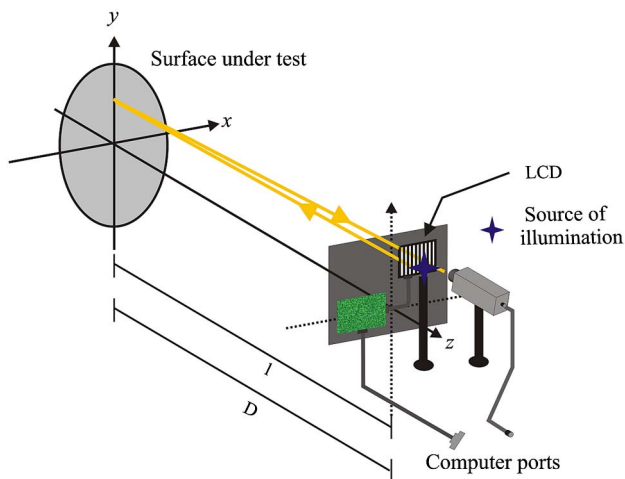

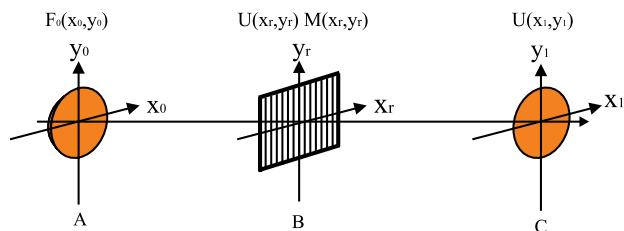Fig. 1. (Color online) Experimental arrangement of the Ronchi test.

Fig. 2. (Color online) Planes to describe the Ronchi test since the point of view of Fourier theory. A, Exit pupil of the surface under test. B, Frequency modulation plane. C, Image plane.

$$F_0(x_0, y_0) = \exp[i2\pi W(x_0, y_0)], \qquad (1)$$

where $W(x_0, y_0)$ denotes the *wavefront deformation function*. The aberration represented by $F_0(x_0, y_0)$ is evaluated with respect to a sphere of radius of curvature r, having its center in the Ronchi ruling. Following the ideas of the papers [13,14], by applying a Fourier transform, the field $U(x_r, y_r)$ immediately before the Ronchi ruling is given by

$$U(x_r, y_r) = \int\int_{-\infty}^{\infty} F_0(x_0, y_0)$$
$$\times \exp\left[-i\frac{2\pi}{\lambda r}(x_r x_0 + y_r y_0)\right] dx_0 dy_0. \quad (2)$$

As the Ronchi ruling is in the Fourier plane the ruling acts as a spatial filter denoted by $M(x_r, y_r)$; under these circumstances, the field immediately after the ruling is given by $U(x_r, y_r)M(x_r, y_r)$. The field in the observation plane, denoted as $G(x_1, y_1)$, is calculated as the inverse Fourier transform of the field in the Ronchi ruling and is given by

$$G(x_1, y_1) = \int\int_{-\infty}^{\infty} U(x_r, y_r)M(x_r, y_r)$$
$$\times \exp\left[i\frac{2\pi}{\lambda r}(x_r x_1 + y_r y_1)\right] dx_r dy_r. \quad (3)$$

As mentioned previously, the Ronchi ruling is composed of straight, equidistant, and parallel bands that can be represented as [12]

$$M(x_r, y_r) = \sum_{n=-\infty}^{\infty} B_n \exp i\frac{2\pi n}{p}x_r, \qquad (4)$$

where p is the ruling period and B_n are the Fourier coefficients assigned to each diffracted order. Finally, by substituting Eqs. (2) and (4) into Eq. (3), and solving the integral, we get

$$G(x_1, y_1) = \sum_{n=-\infty}^{\infty} B_n F_0\left(x_1 + \frac{\lambda r n}{p}, y_1\right), \qquad (5)$$

where r is the paraxial radius of curvature of the optical surface under test. The coefficients are displaced by an amount $\frac{\lambda r n}{p}$.

B. Representation of Ronchigrams

An interferogram can be written as [15]

$$I(x,y) = I_0 + \beta \cos\left[\frac{2\pi}{\lambda} \text{OPD}(x,y)\right], \qquad (6)$$

where $\text{OPD}(x,y)$ is the optical path difference (OPD) between two interfering beams. In a lateral sheared interferometer, the OPD is defined as

$$\text{OPD}(x,y) = \frac{\partial W(x,y)}{\partial x}\Delta x = \alpha(x,y)\Delta x, \qquad (7)$$

where $\alpha(x,y)$ is the wavefront slope, Δx is the lateral shear in the sagittal direction x and $W(x,y)$ represents the aberrated wavefront. As the Ronchi test is a lateral shearing interferometer a Ronchigram can be described through Eq. (6). By employing Eq. (7), we have

$$I(x,y) = I_0 + \beta \cos\left[\frac{2\pi}{\lambda_q}\alpha(x,y)\right], \qquad (8)$$

where $\lambda_q = \frac{\lambda}{\Delta x}$ is a scale factor. The value of Δx represents the lateral displacement, $\frac{\lambda r}{p}$, presented in Eq. (5), r is the paraxial radius of curvature of the optical surface under test, and λ is the capture wavelength of the interferogram. Interferograms are commonly analyzed in normalized coordinates, and due to this fact, Δx will have to be normalized by the maximum radius of the exit pupil of the system; then

$$\Delta'x = \frac{\Delta x}{D/2} = \frac{2\lambda r}{pD}, \qquad (9)$$

where D is the diameter of the exit pupil. After this normalization, λ_q can be written as

$$\lambda_q = \frac{\lambda}{\Delta'x} = \frac{pD}{2r}, \qquad (10)$$

where, in order to produce a change in the phase of the fringes of the Ronchigram due to the wavelength, a low period Ronchi ruling must be employed [16]. Thus, under this condition, the term p in Eq. (10) corresponds to the period of the fringes in the Ronchigram $d(\lambda)$, registered with the wavelength λ, which is defined as [16]

$$d(\lambda) = \frac{\lambda l}{p}, \qquad (11)$$

where l is the distance from the ruling to the surface under test.

C. Ronchigrams with Equivalent Wavelength

The equivalent wavelength intensity pattern is formed by the combination of two rulings with different frequency, as shown in a previous work [11].

These Ronchigrams are obtained with the wavelengths $\lambda_1 \neq \lambda_2$, and can be described by the equations

$$I_1(x,y) = I_{0_1} + \beta_1 \cos\left[\frac{2\pi}{\lambda_{q_1}}\alpha(x,y)\right],$$

$$I_2(x,y) = I_{0_2} + \beta_2 \cos\left[\frac{2\pi}{\lambda_{q_2}}\alpha(x,y)\right]. \qquad (12)$$

In order to generate the Ronchigram with effective wavelength, the intensity functions of Eq. (12) are combined as

$$I_1(x,y)I_2(x,y) = \left\{I_{0_1} + \beta_1 \cos\left[\frac{2\pi}{\lambda_{q_1}}\alpha(x,y)\right]\right\}$$

$$\times \left\{I_{0_2} + \beta_2 \cos\left[\frac{2\pi}{\lambda_{q_2}}\alpha(x,y)\right]\right\}. \qquad (13)$$

The last term of Eq. (13) contains distinct information of the two Ronchigrams, and can be rewritten as

$$\frac{1}{2}\beta_1\beta_2 \cos\left[2\pi\alpha(x,y)\left(\frac{\lambda_{q_2} + \lambda_{q_1}}{\lambda_{q_1}\lambda_{q_2}}\right)\right]$$

$$+ \frac{1}{2}\beta_1\beta_2 \cos\left[2\pi\alpha(x,y)\left(\frac{\lambda_{q_2} - \lambda_{q_1}}{\lambda_{q_1}\lambda_{q_2}}\right)\right]. \qquad (14)$$

The first term of Eq. (14) generates a fringe pattern of equal or higher frequency than the frequencies of the experimental Ronchigrams, while the second term contains the equivalent wavelength. The amount $\frac{\lambda_{q_2} - \lambda_{q_1}}{\lambda_{q_1}\lambda_{q_2}}$ is the scale factor, λ_{qR}, for the Ronchigram with equivalent wavelength, from which the wavelength for the generated pattern, according to Eqs. (10) and (11), is

$$\lambda_{eqR} = \frac{\lambda_1\lambda_2}{\lambda_2 - \lambda_1}, \qquad (15)$$

which is the definition for the equivalent wavelength [1,5,7].

In order to obtain the Ronchigram with equivalent wavelength through the combination of two Ronchigrams as defined by Eq. (13) it is necessary to select the frequency generated by the equivalent wavelength. As the equivalent wavelength is greater than any wavelength in the final pattern, it is necessary to select the cutoff frequency value [17] less than any of the frequencies of the combined Ronchigrams; i.e.,

$$D_0 < \min\left\{f_1 = \frac{1}{\lambda_{q_1}}, f_2 = \frac{1}{\lambda_{q_2}}, f_3 = \frac{1}{\lambda_{q_+}}\right\}, \qquad (16)$$

where, from the first term of Eq. (14), f_3 denotes the frequency generated by the wavelength

$$\lambda_{q_+} = \frac{\lambda_{q_1}\lambda_{q_2}}{\lambda_{q_1} + \lambda_{q_2}}. \tag{17}$$

Then, after a filtering process, we have the pattern

$$I_f(x,y) = I_{0_1}I_{0_2} + \frac{1}{2}\beta_1\beta_2 \cos\left[\frac{2\pi}{\lambda_{qR}}\alpha(x,y)\right], \tag{18}$$

which corresponds to a Ronchigram with the equivalent wavelength λ_{eqR}.

Thus, the process to generate a Ronchigram with equivalent wavelength can be summarized as follows. First, by using an appropriate low period Ronchi ruling [16], two Ronchigrams must be registered, R_1 and R_2 with different wavelengths, λ_1 and λ_2, respectively. Second, by employing Eq. (13), or by implementing the difference between R_2 and R_1, a moiré pattern of these Ronchigrams can be obtained. Finally, as the moiré pattern contains several frequencies, of which the lower corresponds to the equivalent wavelength, a lowpass filter must be employed in order to select the Ronchigram with the equivalent wavelength. Besides these steps, in this paper we show that with proper enhancing algorithms, the results can be significantly improved.

3. Processing of Ronchigrams

Previously, we briefly described the computational methods for the combination of two Ronchigrams in the generation of a Ronchigram with equivalent wavelength [11]. In this work, we describe in a more detailed way the DIP methods employed to generate the Ronchigram with equivalent wavelength and discuss the main difficulties encountered during the process.

A. Gamma-Correction

We found that with appropriate enhancing algorithms of the DIP, applied in the preprocessing stage, the visibility of the fringes in the final Ronchigram can be significantly improved. After the application of a smoothing linear spatial filter for blurring and to bridge small details appearing in the images due to the physical configuration of the LCD, we apply a gamma-correction of the form [17]

$$s = cr^\gamma, \tag{19}$$

where c and γ are positive constants, r is the gray level input, and s is the output. We found that when applying this transformation with values less than 1, around $0.6 \leq \gamma \leq 0.8$, to each Ronchigram before combining them, the visibility in the final pattern is improved. Nonetheless, sometimes the election of $\gamma > 1.0$ has the effect of improving the visibility of those regions of the image that were not enhanced with the mentioned interval; in these cases, we simply proceeded to analyze the images in both intervals and then join them. But for most of the cases, a gamma of less than one worked successfully. In order to observe this effect, Fig. 3 shows the profiles of generated Ronchigrams (after being filtered) when applying two distinct values of gamma to the Ronchigrams to be processed. As can be noted, a considerable improvement of the visibility of the fringes is appreciated
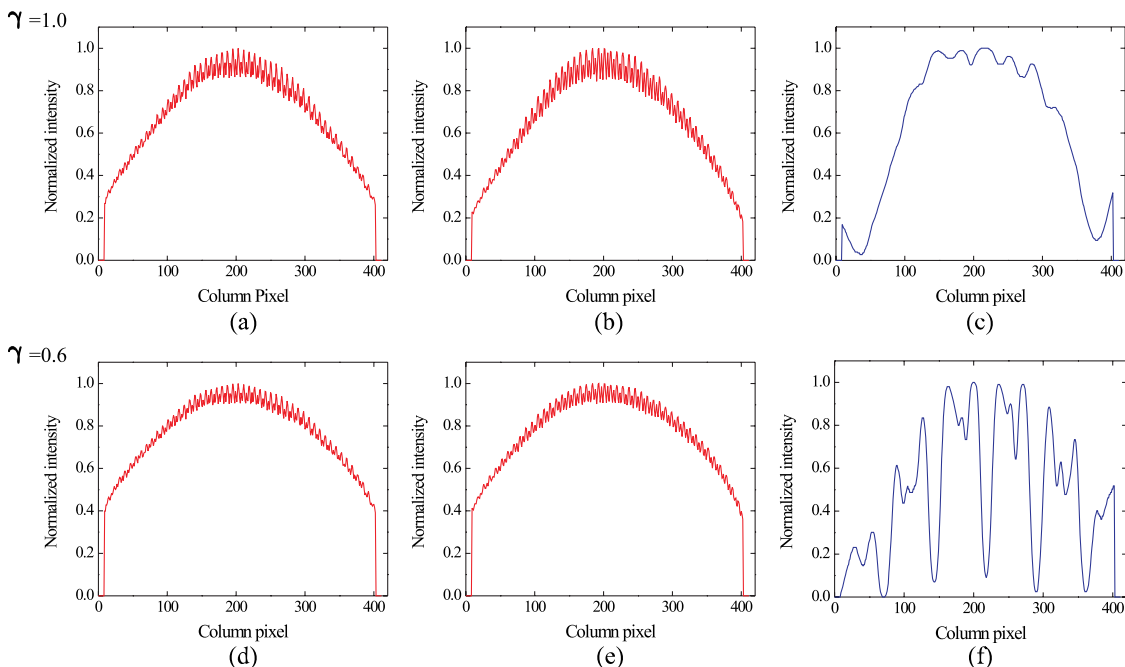

Fig. 3. (Color online) Fringe visibility modification with gamma-correction. (a) and (b) Profiles of Ronchigrams registered with λ_1 and λ_2, respectively, without the application of gamma-correction; (c), profile of the Ronchigram with equivalent wavelength generated with Ronchigrams of (a) and (b). (d) and (e) profiles of Ronchigrams registered with λ_1 and λ_2, respectively, applying the gamma-correction with $\gamma = 0.6$; (f) profile of the Ronchigram with equivalent wavelength generated with Ronchigrams of (d) and (e).
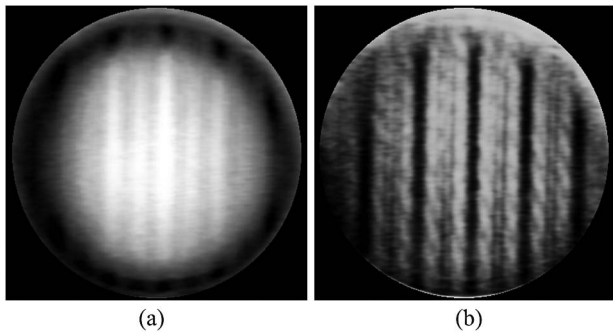
Fig. 4. Ronchigrams with equivalent wavelength modified with gamma-correction. (a) Ronchigram corresponding to the profile shown in Fig. 3(c); (b) Ronchigram corresponding to the profile shown in Fig. 3(f).
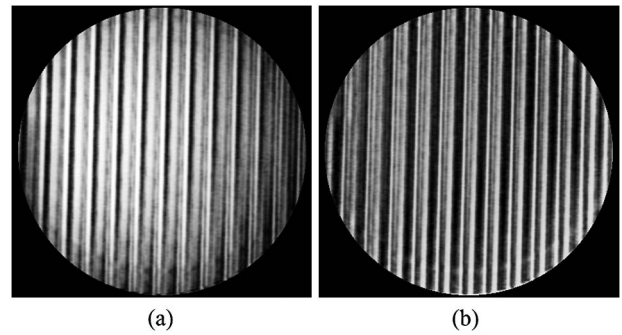

Fig. 5. Improvement of the fringe visibility in Ronchigrams with equivalent wavelength applying distinct values of gamma-correction. (a) $\gamma = 0.8$; (b) $\gamma = 0.2$.

when the gamma-correction is applied. Figure 4 shows the generated Ronchigrams where the previous statement can be confirmed. In fact, as can be noted in Fig. 4(a), sometimes without the application of the enhancement algorithm, the fringes in the Ronchigram are almost null, while, on the other hand, after the application of $\gamma = 0.6$, Fig. 4(b), the fringes are better observed. Figure 5 is another example where the improvement due to the application of the gamma-correction can be seen. For Fig. 5(a), we applied $\gamma = 0.8$, and then by applying lower values of gamma until the value $\gamma = 0.2$, we improved the visibility of the fringes in the final pattern.

We noted that applying the gamma-correction to a Ronchigram before it is combined has an effect of redistributing the intensity along the Ronchigram more homogeneously. This effect can be noted in Fig. 6, where for a given Ronchigram, the profile of its central row is shown for several values of γ. As can be noted in Fig. 6(a) (the Ronchigram without processing), the profile is mounted on the intensity distribution of the source of illumination, and the effect of the application of the gamma-correction, Figs. 6(b) and 6(c), has the effect of extending the intensity distribution of the profile. This intensity redistribution makes the fringe visibility more homogeneous along the Ronchigram, as shown in Fig. 6(c). In this way, when the gamma-correction is applied to the Ronchigrams to be combined, the similarity or coherence between

the Ronchigrams is increased, producing better results, as in the example shown in Fig. 3.

We also noted that the background signal in a Ronchigram increases when the gamma-correction is applied, as shown in Fig. 6(c). This effect also helps to improve the fringe visibility in the generated pattern, because this signal is suppressed in the Ronchigram with equivalent wavelength. In this way, the information in the final pattern corresponds more to the information of the fringes and less to the background. We must state, however, that once we found the adequate value of γ_1, which produced adequate results, the application of a $\gamma_2 < \gamma_1$ does not improve the visibility of the results.

Although gamma-correction is a useful tool for improving the visibility of the Ronchigrams with equivalent wavelength, misalignment problems can affect fringe visibility in the generated patterns [11] A typical misalignment problem appearing in Ronchigrams is the effect known as *vignetting*. This effect moves the maximum illumination outside the center of the image. Then, if two Ronchigrams are registered with certain misalignment, the generated pattern with these Ronchigrams will present null visibility in the darker areas created by the misalignment. However, this problem can be corrected by employing an aperture stop in order to properly align the camera with the converging beam coming from the surface under test such that the maximum intensity is at the center of the Ronchigram [11].
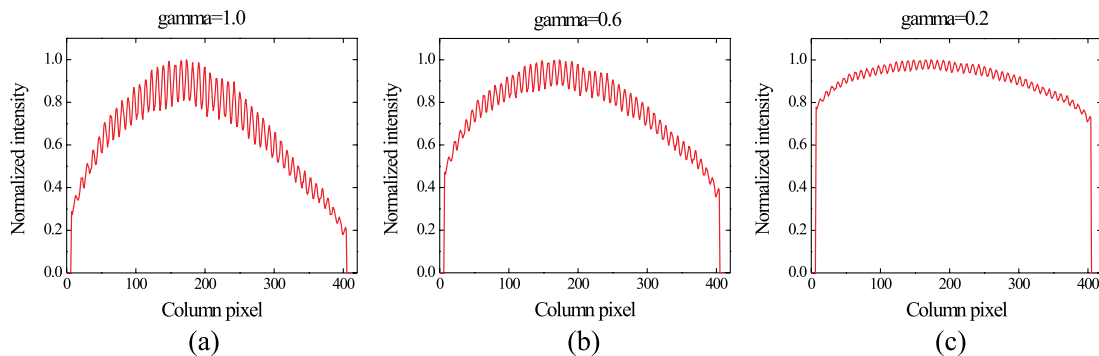

Fig. 6. (Color online) Behavior of the intensity distribution of Ronchigrams due to the application of distinct values of gamma-correction. (a) Without modification, $\gamma = 1.0$; (b) $\gamma = 0.6$; (c) $\gamma = 0.2$.
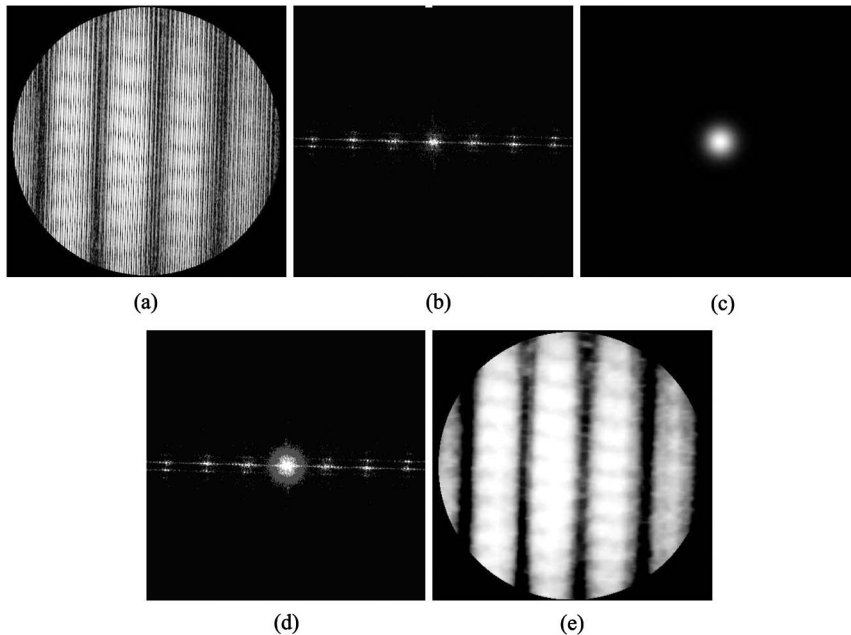
Fig. 7. Filtering process employed in this work. (a) Pattern with equivalent wavelength without filtering; (b), Fourier transform of the pattern in (a); (c), Gaussian filter; (d) filtering of frequencies; (e), filtered pattern with equivalent wavelength.

B. Gaussian Lowpass Filter

As mentioned in Subsection 2.C, a lowpass filter needs to be applied in order to select the pattern belonging to the Ronchigram with equivalent wavelength. In this work, we employed a Gaussian lowpass filter in the frequency domain described by [17]

$$H(u,v) = \exp{-\frac{D^2(u,v)}{2\sigma^2}}, \qquad (20)$$

where $D(u,v)$ is the distance from the origin of the filter to the coordinate (u,v) in the Fourier domain, and σ is a measure of the spread of the Gaussian curve [17]. Usually, $\sigma = D_0$, the cutoff frequency. Then, the selection of the cutoff frequency can be made through Eq. (16) or by displaying the Fourier transform of the pattern that results from the two Ronchigrams, and then by superimposing the filter on this image, we can select the cutoff frequency. This procedure was followed in this work in order to have more control on the selection of the cutoff frequency

as shown in Fig. 7, where we show (a) the combination of two Ronchigrams, (b), the Fourier transform of (a), (c) the Gaussian Filter, (d) the Gaussian filter superimposed on (a), and (e) the result of the filtering. This procedure allowed us to select the value of σ in this work, where for ruling frequencies of [200,350] lines per inch we found that $70 \leq \sigma \leq 110$.

4. Experimental Array and Results

A. Experimental Array

The experimental configuration used in this work is shown in Fig. 8. As mentioned previously, instead of a traditional ruling, we used an LCD in order to display the ruling in any direction. The LCD used in this experiment is a spatial light modulator (XGA2 SLM), which displays binary patterns with a maximum spatial resolution of 1024 × 768 pixels. The dimensions of the active pixels are 23 × 16 μm. In order to observe an image on the LCD, two polarizers rotated 90° were used. The first polarizer was placed on
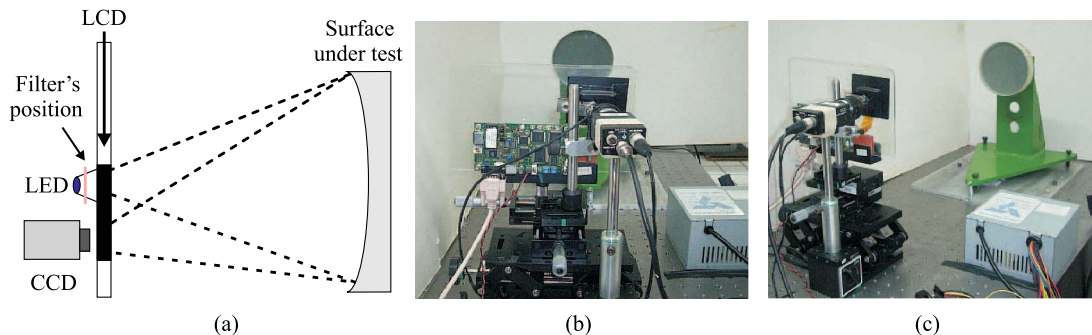

Fig. 8. (Color online) Experimental configuration of the Ronchi test employed in this work. (a) Schematic top view; (b), view from behind; (c) lateral view.
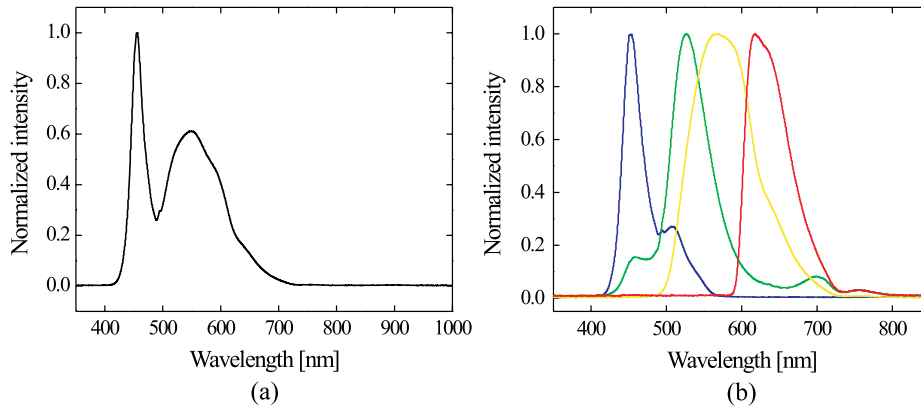
Fig. 9. (Color online) Spectral distribution of the (a) white LED; (b) color filters.

the side that sees the surface under test, and the second one on the opposite side, which corresponds to the observation plane. The illumination source was placed next to the LCD on the side of the observation plane, as shown in Fig. 8(a). Figures 8(b) and 8(c) show some views of the experimental arrangement where the advantage of employing an LCD can be observed because different frequencies or different rulings can be used.

As source of illumination, we employed a white LED, and in order to have different wavelengths, we used colored commercial papers as filters in order to select different wavelengths. The filters are simply placed in front of the LED in order to select the desired wavelength. Figure 9(a) shows the spectral distribution of the white LED, and Fig. 9(b) shows the spectral distribution of four filters. According to Fig. 9(b), the maximum of the spectral distribution for each of these filters are as follows: blue—452.91 nm, green—526.95 nm, yellow—567.80 nm, and red—617.83 nm, which will be the values of λ_1 and λ_2 employed in the computation of the equivalent wavelength, λ_{eq}.

In this work, we tested a spherical mirror with 12.81 cm diameter and 50.0 cm curvature radius with traditional and substructured rulings. Nonetheless, this technique can be applied to a wide variety of optical surfaces. (In fact, due to its versatility, with proper improvements, this proposal could be employed as a tuning system in order to control the

number of fringes of a Ronchigram according to different equivalent wavelengths.). By using the arrangement presented in Fig. 8, several Ronchigrams with traditional and substructured rulings, for different wavelengths, were captured. Figure 10 shows two typical 7 bit substructured Katyl type rulings employed in this work [18], which are employed in the Ronchi test to produce narrower bands in order to obtain more information from a Ronchigram [19–21]. The application of these kinds of sequences to the Ronchi test is analogous to the narrow interference lines of multiple beam interferometry [18].

B. Results

Figure 11 shows the evaluation of the spherical mirror previously mentioned with traditional rulings. All images in this figure are of size 425 × 430 pixels. The size of the pupil, which corresponds to the diameter $D = 12.81$ cm, is of size 420 × 420 pixels. The wavelengths employed in this evaluation were $\lambda_1 = 526.95$ nm, green, and $\lambda_2 = 617.83$ nm, red. The distance from the ruling to the mirror was $l = 46.5$ cm, and the period of the ruling was $p = 156$ μm, i.e., 384 lines per centimeter by employing 3 pixels for a line. Under these conditions, the period of the fringes for the Ronchigram with the green wavelength, Fig. 11(a), is of 1.5707 mm, which corresponds in the image to 5.14 pixels. For the Ronchigram with the red wavelength, Fig. 11(b), the period of the fringes is of 1.841 mm, which corresponds in the image to 6.03 pixels.

These periods were verified according to the profiles of these Ronchigrams shown in Figs. 12(a) and 12(b). The experimental period of the Ronchigram with equivalent wavelength, Fig. 12(c), is around 36 pixels, which, for the values of l and p given previously, corresponds to 1.098 cm and to an equivalent wavelength of 3.68 μm. While the equivalent wavelength calculated with Eq. (15) gives 3.58 μm, which coincides with the experimental wavelength.

Evaluation with a 7 bit substructured Katyl type ruling (Fig. 10) is shown in Fig. 5. A frequency of 54 sequences per centimeter was employed. In this example, the employed wavelengths were blue—452.91 nm and yellow—567.80 nm, for which the

Fig. 10. 7 bit substructured rulings of the Katyl type: (a) positive and (b) negative.
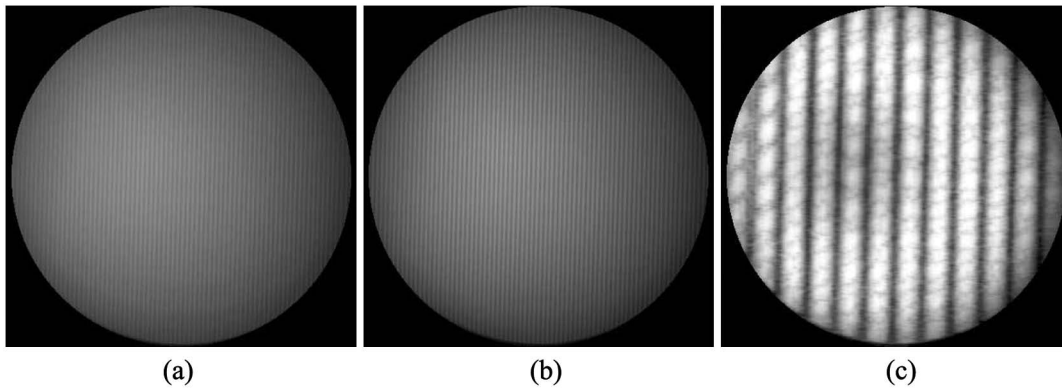
Fig. 11. Generation of a Ronchigram with equivalent wavelength for traditional Ronchi rulings. (a) Ronchigram with λ_1; (b) Ronchigram with λ_2; (c) Ronchigram with λ_{eq}.

equivalent wavelength is $\lambda_{eq} = 2.238$ μm, generating a total of 12 substructured fringes. In order to show the versatility of the system, we also tested the surface with the red—617.83 nm wavelength, which was combined with the yellow wavelength—567.80 nm. The Ronchigrams and the pattern with the equivalent wavelength are presented in Fig. 13, for which the equivalent wavelength is $\lambda_{eq} = 7.011$ μm and the number of substructured fringes is reduced to three fringes, Fig. 13(c). These examples demonstrate the ease of generating patterns with equivalent wavelength with this proposal. Finally, Fig. 14 shows the profile of the Ronchigrams of Fig. 13. As can be observed, the advantages of the results with this proposal are the good visibility of the fringes in the

generated pattern [Fig. 14(c)] and the small increase of the noise in the pattern with equivalent wavelength, which has been reported as one of the main problems with interferometrical techniques [9].

Certain limitations exist with substructured rulings due to the resolution of the LCD. In order to maintain a low period Ronchi ruling to produce a change in the fringes due to the wavelength, the maximum affordable frequency with substructured sequences with the LCD must be used. With 1024 pixels in the horizontal direction of the LCD, the maximum frequency achieved with any 7 bit substructured ruling is around 54 sequences per centimeter by employing one pixel of the LCD per bit. Also, another limitation appears if we try to
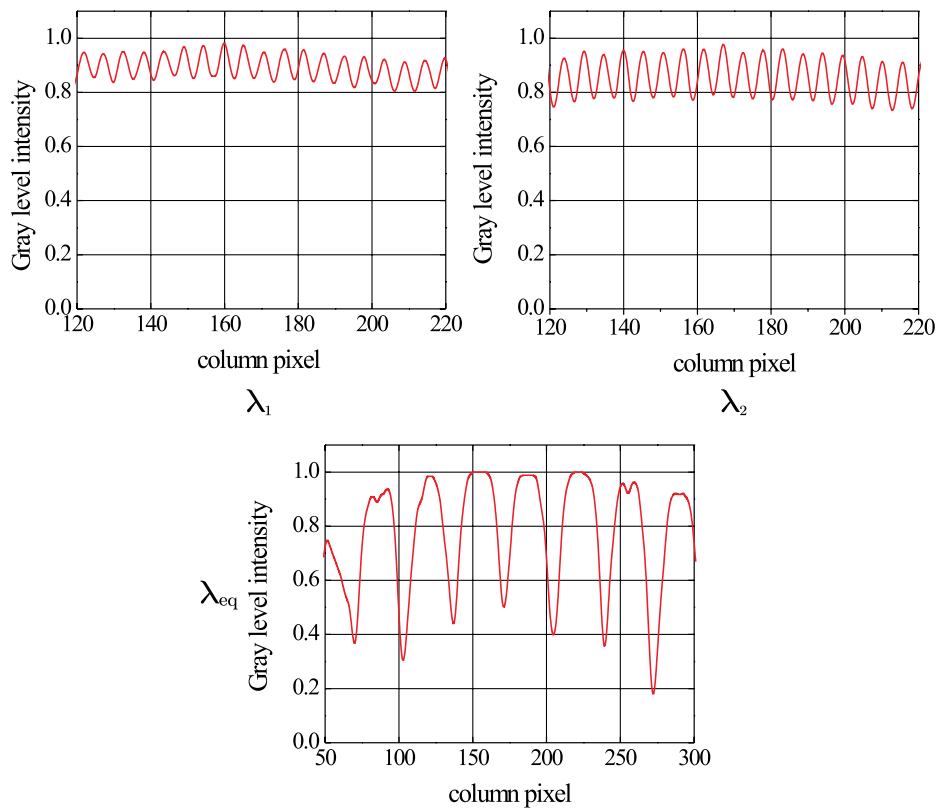

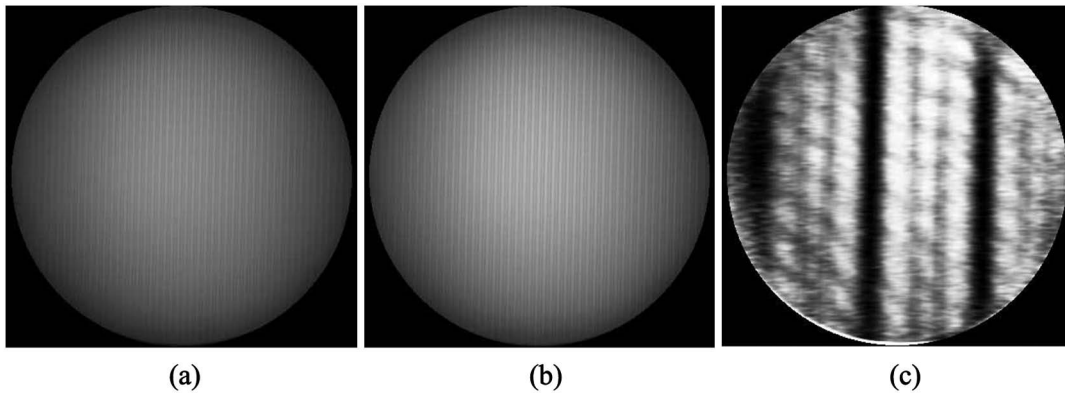Fig. 12. (Color online) Profiles of the central row pixel of Ronchigrams of Fig. 11.

Fig. 13. Generation of a Ronchigram with equivalent wavelength and 7 bit substructured Ronchi rulings. (a) Ronchigram with λ_1; (b) Ronchigram with λ_2; (c) Ronchigram with λ_{eq}.
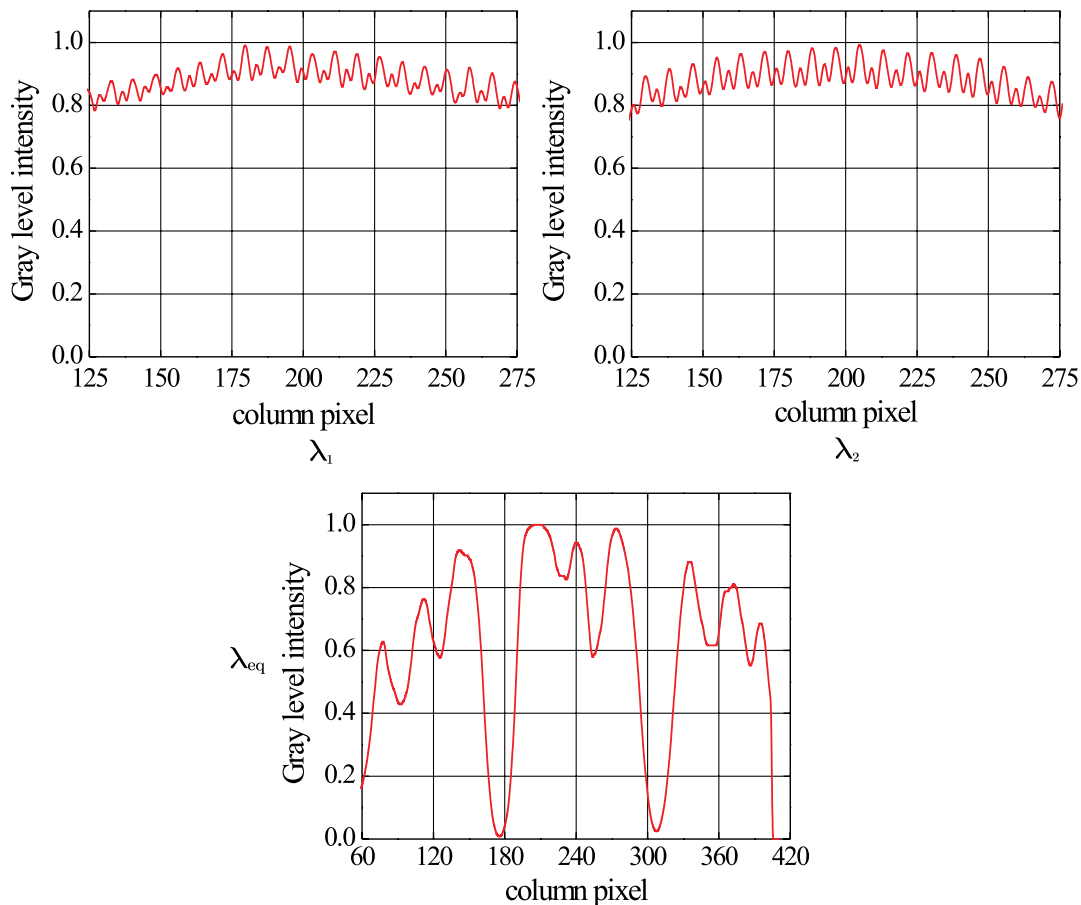

Fig. 14. (Color online) Profiles of the central pixel row of Ronchigrams of Fig. 13.

increase the frequency of the fringes in the Ronchigram by moving the ruling near the paraxial radius of curvature, because beyond a certain limit, the substructure is lost and a binary pattern is observed instead. Then, the employment of the LCD presents some restrictions due to the minimum size of the pixel when working with substructured rulings.

5. Conclusions

In this paper, we have introduced an experimental method based on the Ronchi test along with the concept of equivalent wavelength. We discussed the main ideas of the proposal and showed that with proper image processing algorithms, the visibility of the patterns with equivalent wavelength can be significantly improved. We also discussed some of the main advantages of the proposal, such as the good visibility of the fringes and the low noise in the generated patterns. We showed experimental results (with incoherent light) of the evaluation of a spherical mirror with traditional and 7 bit substructured Ronchi rulings, for which experimental and theoretical

values of the equivalent wavelength agreed. We also presented some of the limitations of the proposal, which we believe can be overcome by the employment of an LCD with smaller pixel size. Finally, we believe that this proposal can be automatized in order to have a more robust technique for the evaluation of infrared surfaces in the optical workshop.

References

1. J. C. Wyant, "Testing aspherics using two-wavelength holography," Appl. Opt. **10**, 2113–2118 (1971).
2. W. B. Ribbens, "Surface roughness measurement by two wavelength holographic interferometry," Appl. Opt. **13**, 1085–1088 (1974).
3. K. Creath, "Step height measurement using two-wavelength phase shifting interferometry," Appl. Opt. **26**, 2810–2816 (1987).
4. J. A MacGovern and J. C. Wyant, "Computer generated holograms for testing optical elements," Appl. Opt. **10**, 619–624 (1971).
5. B. P. Hildebrand and K. A. Haines, "Multiple-wavelength and multiple-source holography applied to contour generation," J. Opt. Soc. Am. **57**, 155–162 (1967).
6. S. J. Zelenka and R. J. Varner, "Multiple-index holographic contouring," Appl. Opt. **8**, 1431–1434 (1969).
7. C. Polhemus, "Two-wavelength interferometry," Appl. Opt. **12**, 2071–2074 (1973).
8. K. M. Leung, T. C. Lee, and G. E. Bernal, "Two-wavelength contouring with the automated thermoplastic holographic camera," Proc. SPIE **0192**, 184–189 (1979).
9. J. C. Wyant, B. F. Oreb, and P. Hariharan, "Testing aspherics using two-wavelength holography: use of digital electronic techniques," Appl. Opt. **23**, 4020–4023 (1984).
10. P. D. Groot and S. Kishner, "Synthetic wavelength stabilization for two-color laser-diode interferometry," Appl. Opt. **30**, 4026–4033 (1991).
11. A. A. Garcia, A. F. S. Granados, and R. A. Cornejo, "Wavefront determination using the Ronchi test with synthetic wavelength," Proc. SPIE **8011**, 8011D-1, (2011).
12. A. R. Cornejo, "Ronchi test," in *Optical Shop Testing*, D. Malacara, ed. (Wiley Interscience 2007), pp. 317–360.
13. J. L. Rayces, "Exact relation between wave aberration and ray aberration," Opt. Acta **11**, 85–88 (1964).
14. R. Barakat, "General diffraction theory of optical aberration tests, from the point of view of spatial filtering," J. Opt. Soc. Am. **59**, 1432–1439 (1969).
15. W. S Meyers and H. P. Stahl, "Sensitivity of two-channel Ronchi test to grating misalignment," Proc. SPIE **1994**, 90–101 (1994).
16. A. Cornejo and D. Malacara, "Ronchi test of aspherical surfaces, analysis, and accuracy," Appl. Opt. **9**, 1897–1901 (1897).
17. R. C. Gonzalez and R. E. Woods, *Digital Image Processing*, 3rd ed. (Prentice Hall, 2008).
18. R. H. Katyl, "Moiré screens coded with pseudo-random sequences," Appl. Opt. **11**, 2278–2285 (1972).
19. L. Yaoltzin and Z. Yaoltzin, "Prueba de Ronchi con rejillas sub-estructuradas," Master's thesis (INAOE, 2005).
20. G. M. Campos and A. F. Granados, "Interferometric Ronchi test by using sub-structured gratings," Proc. SPIE **7390**, 73901B (2009).
21. L. J. Salinas, A. F. Granados, R. A. Cornejo, E. Luna, J. J. E. Sánchez, and J. M. C. Hernández, "Ronchi test with variable-frequency rulings," Opt. Eng. **48**, 013604 (2009).